Passive Scalar Transport in Coaxial-Swirling Jets

o Pravin Ananta Kadu, Dept. of Mechanical Science and Engineering, Nagoya University, Furo-cho, Chikusa-ku, Nagoya 464-8603, E-mail: kadu.pravin.ananta@h.mbox.nagoya-u.ac.jp
Yasuhiko Sakai, Dept. of Mechanical Systems Engineering, Nagoya University
Yasumasa Ito, Dept. of Mechanical Systems Engineering, Nagoya University
Koji Iwano, Dept. of Mechanical Systems Engineering, Nagoya University
Masatoshi Sugino, Dept. of Mechanical Systems Engineering, Nagoya University
Takahiro Katagiri, Information Technology Center, Nagoya University

A direct numerical simulation (DNS) of coaxial jets with a strong swirl has been carried out and the mixing characteristics have been investigated with the help of two separate passive scalars injected from the jets. A case of coaxial jets without swirl is also considered for the comparison purpose. The strongly swirling case develops an internal recirculation zone (IRZ), which results into the enhanced radial outward flux of inner jet scalar concentration as well as the faster rate of inward spread of outer jet scalar concentration. This results into an early mixing of jets in swirling case as compared to that in non-swirling case.

1. Introduction

Swirl jets are widely used in the industrial burners because of its characteristics: increase in jet growth and rate of decay of the jet(1). In addition to this, the strong swirl creates an adverse pressure gradient, setting up the internal recirculation zone (IRZ)(2). This prevents the flame from blowing out as well as recirculates the heated products of combustion which helps to ignite the incoming fuel/oxidant jets. Although some attention has been given to the scalar mixing(3-4), the mixing mechanism is needed to be examined extensively. The focus of present study is to investigate the mixing enhancement in coaxial-swirling jets with the help of two passive scalars injected from both jets.

2. Numerical setup

Fig. 1 shows the schematic of the inlet nozzle configuration and the computational domain. The axis of nozzle coincides with the *x*-axis (streamwise direction. The nozzle configuration is presented in terms of inner jet diameter *D*.

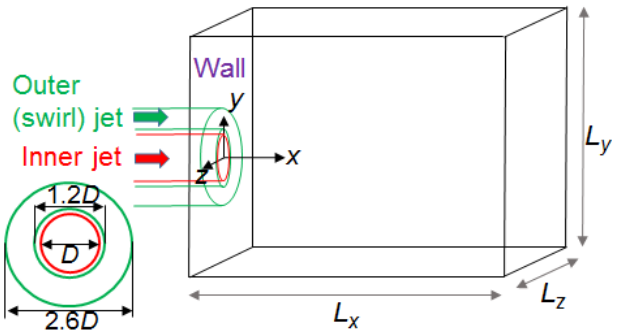

Fig. 1 Schematic of the nozzle configuration and computational domain.

The governing equations used for the fluid flow are incompressible Navier-Stokes equation and the continuity equation while the diffusion equation is used for the passive scalar concentration. These equations are solved using fractional step method and the pressure Poisson equation is solved using conjugate gradient method. The 2nd order Runge-Kutta method is used for the time iterations. The uniform Cartesian grid is employed with 4th order spatial discretization scheme in *x*-direction and 2nd order in *y* and *z* directions. Neumann boundary condition is considered in *y* and *z* directions. Convective outflow boundary condition is employed at the outlet.

The precursor simulations for nozzle were performed using the OpenFOAM code to generate the inflow mean velocity profiles along with their fluctuations. The mean flow rate ratio and the cross-sectional averaged velocity ratio between outer and inner pipe flows are 10.64 and 2.0 respectively. Reynolds number of inner pipe flow is 2200. The swirl in the outer jet is generated from four upstream vanes. Instantaneous velocity components at the outlet of nozzle are then given to the DNS inlet. The swirl number which measures the intensity of swirl is calculated at the nozzle exit by formula,

$$Sw = \left[\int_0^{R_0} \overline{U}\,\overline{V_\theta} r^2 dr\right] \Big/ \left[R_0 \int_0^{R_0} \left(\overline{U}^2 - \overline{V_\theta}^2/2\right) r dr\right] \quad \text{(a)}$$

where R_0 is the outer radius of outer jet and $\overline{*}$ denotes the time average. Two cases are considered: (I) without vanes: *Sw*=0, and (II) with vanes: Sw=1.8. Separate passive scalars are injected from inner jet (IJ) and outer jet (OJ). Top-hat profile is given to the scalar concertation at the nozzle exit and Schmidt number is equal to 1.

The DNS domain size taken for non-swirling case is 20*D*×20*D*×20*D* with the grid size 701×701×701, while that for swirling case is 20*D*×28*D*×28*D* with the grid size 701×981×981. The results are represented in the cylindrical coordinate system.

3. Evolution of mean scalar concentrations

Figure 2 shows the contour plots for mean of inner jet scalar concentration for both non-swirling and swirling cases. In non-swirling case, the concentration at the centerline starts to decay from around $x \approx 3.0D$ with a slow decay rate in the downstream. Radial spread of the scalar concentration is also seen to be negligible. Contrary to this, swirling case sees the higher rate of scalar concentration decay. The rapid decrement of

scalar concentration is started from $x < 2.0D$ and is a result of partially-penetrated vortex breakdown bubble[5] or simply internal recirculation zone (the leading stagnation point on the centerline is placed at $x \approx 2.5D$), where the recirculation flow acts as a barrier. The annular reversed flow between the inner and outer jet ($0 < x/D < 2.0$) increases the radial outward scalar flux, causing the inner jet scalar to spread radially outward. The concentration is observed to be negligible $x \approx 6.5D$ onwards.

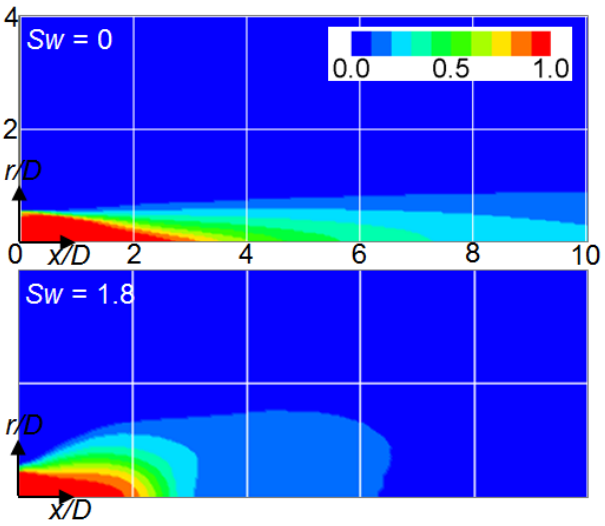

Fig. 2 Contours of mean of inner jet (IJ) scalar concentration.

Figure 3 shows the contour plots for mean of outer jet scalar concentration for both non-swirling and swirling cases. The maximum outer jet scalar concentration in the non-swirling case is seen to be extended until $x \approx 3.0D$, while the scalar reaches to the centerline by $x \approx 3.0D$. In case of strong swirl, the scalar concentration starts to decay earlier with the maximum concentration extending until $x \approx 1.0D$. Radial spread of the scalar concentration at the same time is enhanced with it reaching to the centerline by $x \approx 2.0D$.

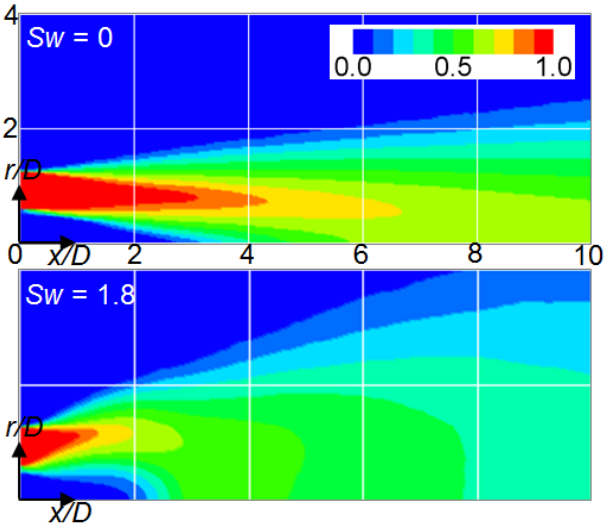

Fig. 3 Contours of mean of outer jet (OJ) scalar concentration.

By comparing the contours of inner jet and outer jet scalar concentrations for each case, it can be observed that the swirling case sees an early mixing of two streams in contrast to the non-swirling case, which lacks the radial flux of scalars in the upstream region ($x < 2.0D$).

4. Conclusion

The present study is evident that the strongly swirling coaxial jets are favorable for enhancing the mixing of two streams as compared to the non-swirling case, where two streams exhibit the slower rate of spread. The internal recirculation zone is seen to be responsible for bounding the scalars close to the nozzle exit. Application-wise, this prevents the burner flame from blowing out and recirculating the combustion products, thus increasing the combustion efficiency.

5. Acknowledgement

The simulations were carried out on Fujitsu PRIMEHPC FX100 and Fujitsu PRIMERGY CX400/270 (Information Technology Center, Nagoya University). This work was supported by JSPS KAKENHI Grant No. 18H01369.

Bibliography

(1) Ribeiro, M. M., and J. H. Whitelaw. "Coaxial jets with and without swirl." Journal of Fluid Mechanics, 96.4 (1980), pp. 769-795.
(2) Champagne, F. H., and S. Kromat. "Experiments on the formation of a recirculation zone in swirling coaxial jets." Experiments in Fluids, 29.5 (2000), pp. 494-504.
(3) Fröhlich, J., M. García-Villalba, and W. Rodi. "Scalar mixing and large-scale coherent structures in a turbulent swirling jet." Flow, Turbulence and Combustion, 80.1 (2008), pp. 47-59.
(4) Ranga Dinesh, K. K. J., Mark A. Savill, Karl W. Jenkins, and M. P. Kirkpatrick. "Large eddy simulation of a turbulent swirling coaxial jet." Progress in Computational Fluid Dynamics, an International Journal, 10.2 (2010), pp. 88-99.
(5) Santhosh, R., Ankur Miglani, and Saptarshi Basu. "Transition in vortex breakdown modes in a coaxial isothermal unconfined swirling jet." Physics of Fluids, 26.4 (2014), p. 043601.